Supplementary Information

Combining Cu-SSZ-13 with TiO_2: Promotion on urea decomposition and influence on SCR

Yue Ma[a], Zhimin Shao[c], Xiaodong Wu[a,*], Yang Gao[a], Baofang Jin,[d] Rui Ran[a], Zhichun Si[b], Zhenguo Li[e], Duan Weng[a,b,*]

[a] *The Key Laboratory of Advanced Materials of Ministry of Education, School of Materials Science and Engineering, Tsinghua University, Beijing 100084, China*

[b] *Graduate School at Shenzhen, Tsinghua University, Shenzhen 518055, China*

[c] *Department of Electronic Engineering, Tsinghua University, Beijing 100084, China*

[d] *State Key Laboratory of Multiphase Complex Systems, Institute of Process Engineering, Chinese Academy of Sciences, Beijing, 100190, China*

[e] *National Engineering Laboratory for Mobile Source Emission Control Technology, China Automotive Technology & Research Center Co., Ltd., Tianjin 300300, China*

The TG curves of the catalysts loaded with urea are shown in Fig. S1 and the weight loss stages are divided according to Figs. 1 and 2. Though the urea loading and water content were slightly different over these catalysts, the contribution of the first urea desorption stage (urea thermolysis) to the overall decomposition weight loss was roughly estimated in Table S1. Ti modification increases the proportion of decomposed urea in the first stage. As a result, the amount of residual urea that transforms to polymerized by-products (*e.g.*, biuret and CyA) at higher temperatures is reduced. The abnormal decreased "F" value over 10Ti-Cu-SSZ-13 is plausibly attributed to decreased Ti dispersion at this high Ti loading.

* Corresponding author. Tel.: +86 10 62792375

E-mail address: wuxiaodong@tsinghua.edu.cn (X. Wu), duanweng@tsinghua.edu.cn (D. Weng)

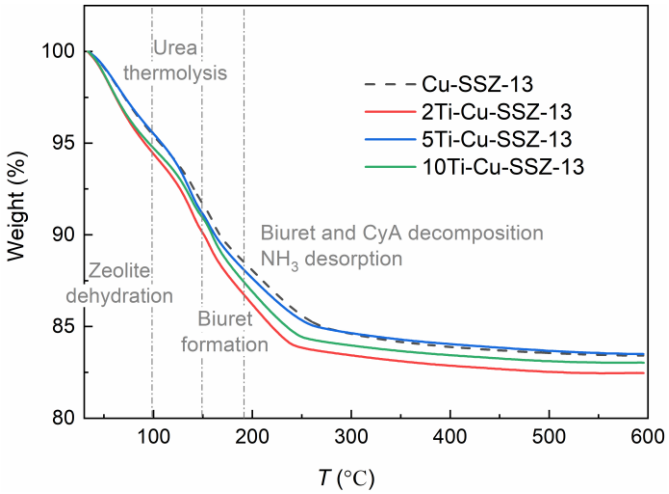

Fig. S1. TG curves of the catalysts loaded with urea.

Table S1. Calculation of the contribution of urea thermolysis in overall decomposition process.

Catalyst	A Total weight loss (%)	B Weight loss after dehydration (%)	C=A-B Urea loading (%)	D Weight loss after urea thermolysis (%)	E=B-D Weight loss of urea thermolysis (%)	F=E/C Proportion of urea thermolysis in total urea loading (%)
Cu-SSZ-13	82.92	95.16	12.48	91.60	3.56	28.5
2Ti-Cu-SSZ-13	82.46	94.50	12.04	90.08	4.42	36.7
5Ti-Cu-SSZ-13	83.50	95.64	12.14	91.20	4.44	36.6
10Ti-Cu-SSZ-13	83.04	94.81	11.77	91.01	3.80	32.3

The N_2 selectivity of the catalysts in SCR tests were calculated according to Eq. S1 and summarized in Fig. S2. All the catalysts show N_2 selectivity close to 100% in the whole temperature range, with N_2O outlet concentration lower than 10 ppm.

$$N_2\ \text{selectivity}\,(\%) = \left(1 - \frac{[NO_2]_{out} + 2\times[N_2O]_{out}}{[NO]_{in} + [NH_3]_{in} - [NO]_{out} - [NH_3]_{out}}\right)\times 100 \qquad \text{(Eq. S1)}$$

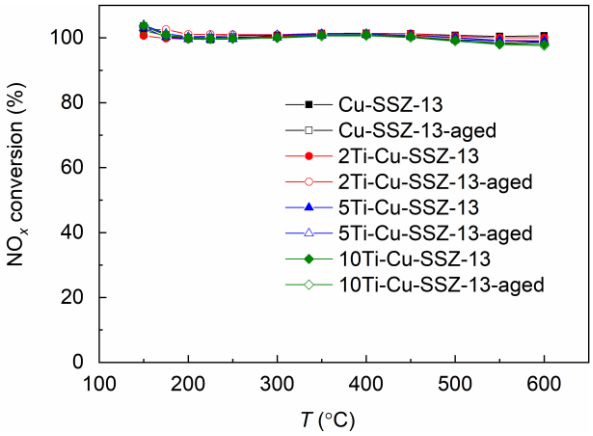

Fig. S2. N_2 selectivity of the catalysts in SCR tests.

Fig. S3 shows the XRD patterns of the catalysts in 2θ range 5-40 ° with a scanning rate of 6 °/min, which exhibit typical CHA diffraction features. Characteristic peaks of TiO_2 can hardly be identified from these fast-scanning curves, indicating high dispersion of TiO_2 nanoparticles. Delicate analysis of TiO_2 structure is provided in the main text (Fig. 6b). Aging does not lead to any remarkable changes on the crystalline structure of the catalysts, except for slightly decreased diffraction intensity due to dealumination.

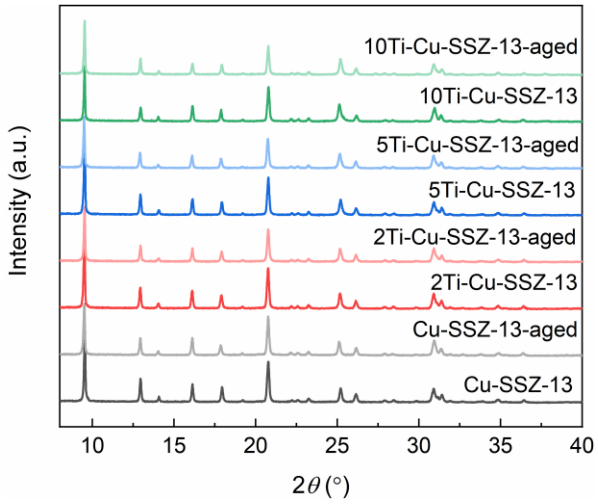

Fig. S3. XRD patterns of the catalysts.

N_2 physisorption experiments (at -196 ℃) was conducted on a JW-BK122F physisorption analyzer (Jingweigaobo, China). The samples were degassed at 220 ℃ for 8 h under vacuum conditions. The specific surface area (S_{BET}) was calculated by Brunauer-Emmett-Tellerand (BET) method, and micropore volume (V_{micro}) was calculated by *t*-plot method.

As listed in Table S2, TiO_2 loading partially blocks the micropores of Cu-SSZ-13, resulting in somewhat decreased S_{BET} and V_{micro}, especially for 10Ti-Cu-SSZ-13. Hydrothermal aging also decreases the S_{BET} and V_{micro} of the catalysts, attributed to partial structural damage. However, such extent of changes in textural properties should not lead to any remarkable differences in SCR and NH_3 oxidation activities (Figs. 3 and 7a).

Table S2. Textural properties of the catalysts.

Catalyst	S_{BET} (m^2/g)	V_{micro} (cm^3/g)
Cu-SSZ-13	762	0.289
2Ti-Cu-SSZ-13	707	0.266
5Ti-Cu-SSZ-13	722	0.272
10Ti-Cu-SSZ-13	634	0.237
Cu-SSZ-13-aged	746	0.266
5Ti-Cu-SSZ-13-aged	711	0.286

NH_3 temperature-programmed desorption (NH_3-TPD) was performed on a fixed bed reactor with a Nicolet 380 (ThermoFisher, USA) FTIR gas analyzer. 50 mg catalyst was loaded and pretreated in 21% O_2/N_2 at 600 ℃ for 20 min. After being saturated in 500 ppm NH_3/N_2 at 100 ℃, sample temperature was ramped to 600 ℃ at a rate of 10 ℃/min. The obtained NH_3-TPD curves are shown in Fig. S4. The desorption of NH_3 can be divided into three stages, originating from weak (<180 ℃), moderate (~200 ℃) and strong (260-600 ℃) acid sites, respectively. Weak and moderate acid sites are assigned to terminal hydroxyls, extraframework Al (EFAl) and Cu ions, while strong acid sites are Si-O(H)-Al bridging hydroxyls. Dealumination already takes place over the parent Cu-SSZ-13 during the 650 ℃ degreening treatment, so the catalyst does no exhibit a large amount of strong acid sites compared to "fresh" catalysts in previous reports.[1, 2] The acid strength and density of TiO_2 are much lower than those of SSZ-13, so Ti modification does not lead to significant change in catalyst acidity, except somewhat decreased amount of total acid sites due to surface coverage by TiO_2.[3] 800 ℃ hydrothermal aging further decreases the amount of strong acid sites and increases those of weak and moderate acid sites due to dealumination.[1, 4] Ti modification does not change the profile of acidity evolution of Cu-SSZ-13 upon aging.

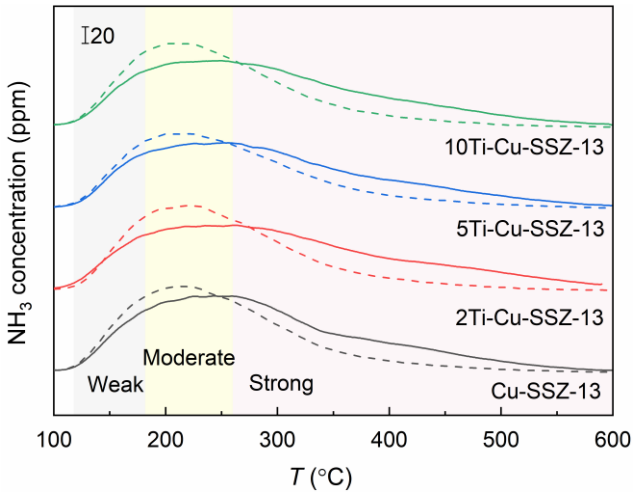

Fig. S4. NH_3-TPD curves of the catalysts. Solid line: fresh; dash line: aged.

Reference TiO_2 material (Alladin, China) was anatase powders with an average diameter of 60 nm. The TiO_2 powders were impregnated with $CuAc_2$ (Sinopharm, China) and calcined at 600 ℃ for 2 h to obtain a sample denoted as CuO/TiO_2-IM. The copper loading was set at 2 wt.%. Fig. S5 shows the UV-vis spectra of these reference samples and Cu-SSZ-13. The adsorption edge of anatase slightly red-shifted after Cu impregnation, and pre-edge feature attributed to Cu-O-Ti charge transfer can be clearly identified over CuO/TiO_2-IM.[5] Bulk CuO contributes to elevated background intensity between 400 and 600 nm. Feature of Cu(II) d-d transfer at ~800 nm also exists on this sample.

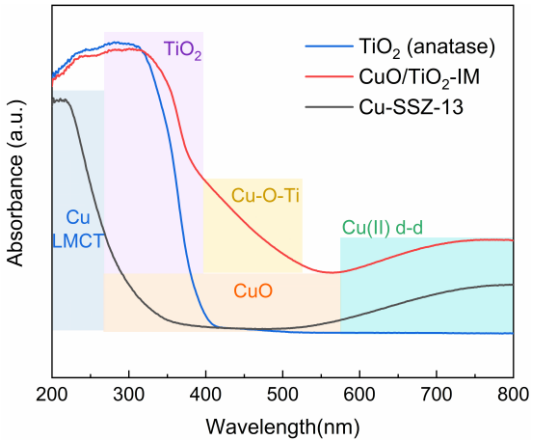

Fig. S5. UV-Vis spectra of the reference samples.

CuO/TiO_2-IM and pure anatase TiO_2 were characterized by H_2-TPR (Fig. S6). TiO_2 exhibits a broad reduction peak at 525 ℃ and continuous H_2 consumption at temperatures higher than 800 ℃, attributed to the reduction of Ti^{4+} (or in other words, lattice O) on surface and in bulk, respectively.[6] Three main H_2 consumption peaks can be identified over CuO/TiO_2-IM. The ones at 125 and 200 ℃ are assigned to the reduction of CuO clusters on TiO_2 with different dispersions (*i.e.*, Cu/TiO_2 in the main text).[7, 8] The one at 350 ℃ is attributed to the reduction of surface Ti^{4+} of TiO_2 activated by Cu.[8, 9] The H spillover effect from Cu to TiO_2 shifts the reduction process towards lower temperatures by ~ 175 ℃.

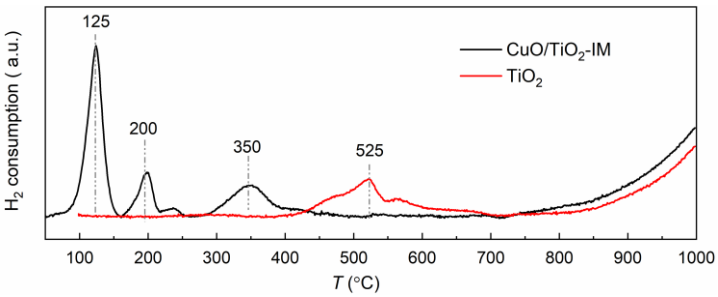

Fig. S6. H_2-TPR of TiO_2 and Cu/TiO_2-IM.

The SCR and NH_3 oxidation activities of CuO/TiO_2-IM are shown in Fig. S7. It has inferior low-temperature SCR and NH_3 oxidation activities compared with Cu-SSZ-13 (Fig. 3). At temperatures above 350 ℃, a negative NO_x conversion of SCR is obtained according to Eq. 1 because the outlet NO_x (*i.e.*, NO, NO_2 and N_2O, mainly NO and NO_2) concentration is higher than the inlet NO concentration (500 ppm). It means that inlet NH_3 is over-oxidized to NO_x under the SCR condition. It is confirmed by NH_3 oxidation test that NH_3 is dominantly converted to NO_x (mainly NO and NO_2) at high temperatures.

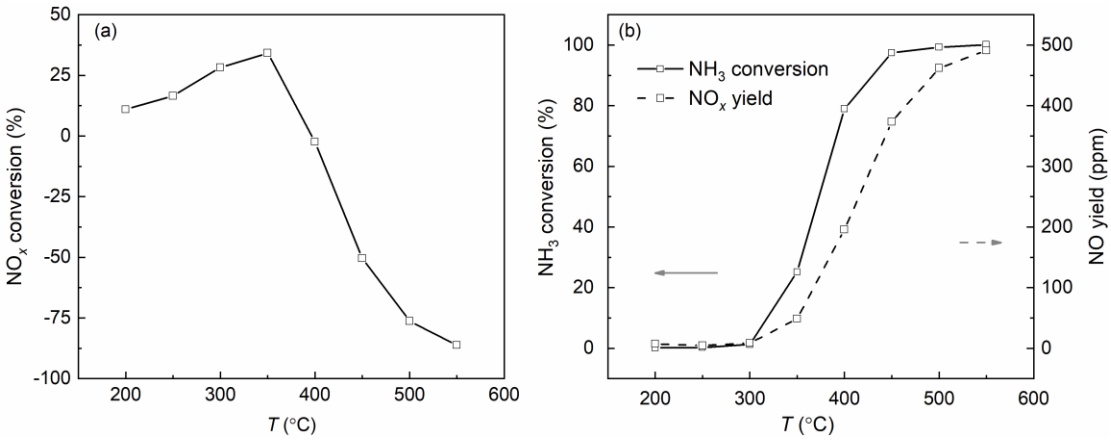

Fig. S7. (a) SCR and (b) NH_3 oxidation activities of CuO/TiO_2-IM. NO yield during NH_3 oxidation is also shown in (b) as dashed lines (right axis). Reaction conditions: 500 ppm NO (w/o)/ 500 ppm NH_3/5% O_2/3% H_2O/N_2, GHSV = 120,000 h^{-1}.

The DTG curves of TiO_2 with urea are shown in Fig. S8. In comparison with fresh TiO_2, 800 ℃ hydrothermally aged TiO_2 exhibits higher onset temperature of urea decomposition and more obvious weight loss features attributed to the decomposition of biuret and CyA (>160 ℃) due to phase transformation from anatase to rutile and sintering of TiO_2.

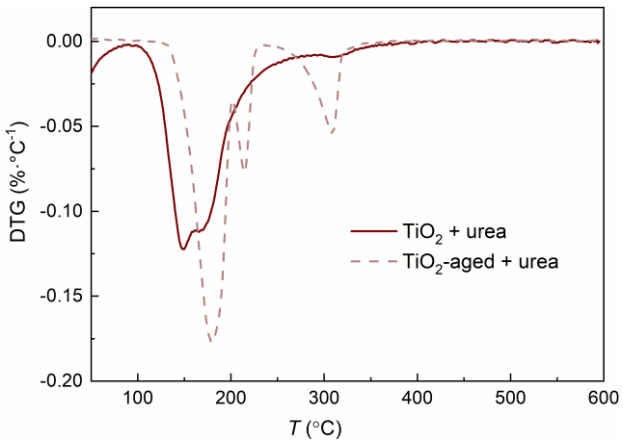

Fig. S8. DTG curves of TiO_2 loaded with urea

Hydrothermal aging decreases the NH_3 oxidation activity of Cu-SSZ-13-aged (Fig. S9), while 5Ti-Cu-SSZ-13-aged exhibits a similar activity to its fresh counterpart. All the aged catalysts show similar NH_3 conversion. NO is the only detectable by-product from NH_3 oxidation, and its yield increases after aging, except that 10Ti-Cu-SSZ-13-aged exhibits less NO formation than its fresh counterpart. Again, all the aged catalysts give similar NO yield. Over Ti-modified catalysts, it is deduced that Cu/TiO_2 species catalyzes the nonselective oxidation of NH_3 to NO in fresh state (Figs. 3b and S7), and this species transforms to CuO- and $CuAl_2O_4$-like species upon hydrothermal aging (Fig. 7d). CuO-like species seems to be more active in nonselective oxidation of NH_3 than Cu/TiO_2, leading to degradation in high-temperature SCR over aged Ti-modified catalysts (Fig. 7a).

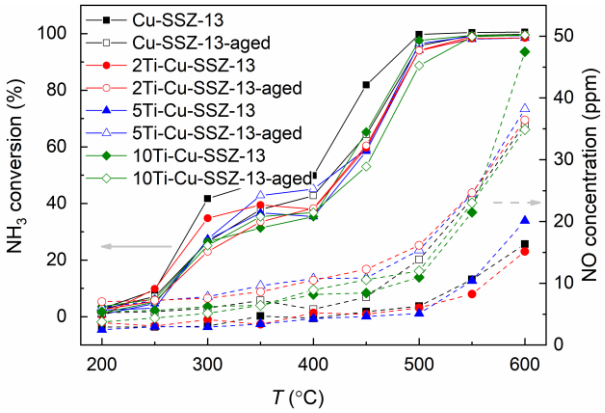

Fig. S9. NH_3 oxidation activities of the catalysts. NO yield during NH_3 oxidation is also shown as dashed lines (right axis). Reaction conditions: 500 ppm NH_3/5% O_2/3% H_2O/N_2, GHSV = 120,000 h^{-1}.

The H_2-TPR curves of all the four aged catalysts are shown in Fig. S10. As discussed in the main text, Cu/TiO_2 species in fresh 5Ti-Cu-SSZ-13 and 2Ti-Cu-SSZ-13 disappears after aging and CuO-like species forms. Due to the similarity in Cu species, 2Ti-Cu-SSZ-13-aged and 5Ti-Cu-SSZ-13-aged act similarly to Cu-SSZ-13-aged in activity tests (Figs. 7a and S9). 10Ti-Cu-SSZ-13-aged still contains Cu/TiO_2 but with a largely decreased amount compared with fresh 10Ti-Cu-SSZ-13, and has the lowest amount of CuO-like species among the aged catalysts. During aging, there probably exists a competition between Cu/TiO_2 and CuO-like species. CuO may have a higher affinity to Cu than TiO_2 does, so CuO-like species grows at the expense of Cu/TiO_2, but the high TiO_2 loading of 10Ti-Cu-SSZ-13-aged may affect such a competition and inhibit the formation of CuO-like species. Besides, Cu/TiO_2 may also transform to inert $CuAl_2O_4$-like species due to the strong affinity of Al_2O_3 to Cu suggested by DFT calculations.[2] Thus, the nonselective oxidation of NH_3 to NO is inhibited over 10Ti-Cu-SSZ-13-aged and the high-temperature SCR activity is somewhat improved compared with fresh 10Ti-Cu-SSZ-13.

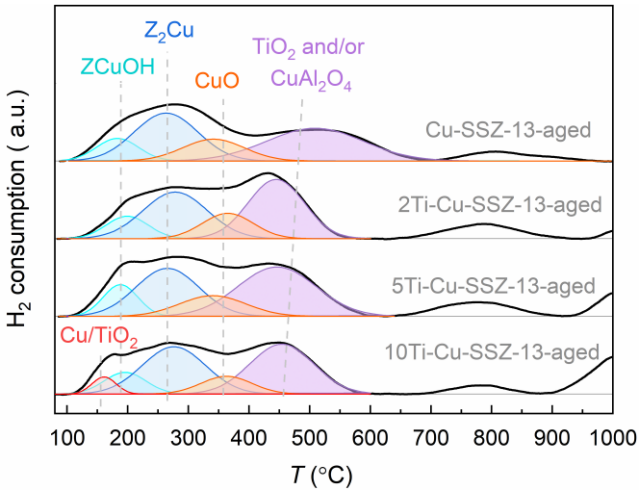

Fig. S10. H_2-TPR of the aged catalysts.

References:

1. Y. Ma, X. Wu, S. Cheng, L. Cao, L. Liu, Y. Xu, J. Liu, R. Ran, Z. Si and D. Weng, *Appl. Catal. A*, 2020, **602**, 117650.
2. Y. Ma, S. Cheng, X. Wu, T. Ma, L. Liu, B. Jin, M. Liu, J. Liu, R. Ran, Z. Si and D. Weng, *J. Catal.*, 2022, **405**, 199.
3. J. Liu, J. Liu, Z. Zhao, Y. Wei, W. Song, J. Li and X. Zhang, *Ind. Eng. Chem. Res.*, 2017, **56**, 5833.
4. D. Wang, Y. Jangjou, Y. Liu, M. K. Sharma, J. Luo, J. Li, K. Kamasamudram and W. S. Epling, *Appl. Catal. B*, 2015, **165**, 438.
5. O. V. Komova, A. V. Simakov, V. A. Rogov, D. I. Kochubei, G. V. Odegova, V. V. Kriventsov, E. A. Paukshtis, V. A. Ushakov, N. N. Sazonova and T. A. Nikoro, *J. Mol. Catal. A*, 2000, **161**, 191.
6. Y. Zeng, Y. Wang, S. Zhang and Q. Zhong, *Phys. Chem. Chem. Phys.*, 2018, **20**, 22744.
7. H. Li, S. Wu, L. Li, J. Wang, W. Ma and K. Shih, *Catal. Sci. Technol.*, 2015, **5**, 5129.
8. X. Wang, X. Chen, L. Ye, P. Lu, Y. Liu, J. You, W. Zeng, L. Lu, C. Hu and D. Chen, *Mol. Catal.*, 2020, **497**, 111225.
9. J. Xiaoyuan, D. Guanghui, L. Liping, C. Yingxu and Z. Xiaoming, *J. Mol. Catal. A*, 2004, **218**, 187.